Inorganic Chemistry

Communication

pubs.acs.org/IC

A New FeMo Complex as a Model of Heterobimetallic Assemblies in Natural Systems: Mössbauer and Density Functional Theory Investigations

Solène Bouchard,[†] Martin Clémancey,[‡,§] Geneviève Blondin,*[,‡,⊥] Maurizio Bruschi,*[,¶] Kévin Charreteur,[†] Luca De Gioia,[∥] Christine Le Roy,[†] François Y. Pétillon,[†] Philippe Schollhammer,*[,†] and Jean Talarmin[†]

[†]UMR CNRS 6521, Université de Bretagne Occidentale, Brest, France

[‡]CEA, iRTSV-LCBM-PMB, 17 rue des Martyrs, 38000 Grenoble, France

[§]Université de Grenoble Alpes, iRTSV-LCBM-PMB, 17 rue des Martyrs, 38000 Grenoble, France

[⊥]CNRS, iRTSV-LCBM-PMB, 17 rue des Martyrs, 38000 Grenoble, France

[∥]Department of Biotechnology and Bioscience, University of Milano-Bicocca, Piazza della Scienza 2, 20126 Milan, Italy

[¶]Department of Earth and Environmental Sciences, University of Milano-Bicocca, Piazza della Scienza 1, 20126 Milan, Italy

Supporting Information

ABSTRACT: The design of the new FeMo heterobimetallic species $[FeMo(CO)_5(\kappa^2\text{-dppe})(\mu\text{-pdt})]$ is reported. Mössbauer spectroscopy and density functional theory calculations give deep insight into the electronic and structural properties of this compound.

The design of bimetallic species has been developed for several decades with the aim of achieving efficient catalysts via a cooperative activation by adjacent metals.[1] In this context, heterobimetallic systems are of interest because of the possible synergistic effects between the two different metal centers that could enhance the activities of such systems.[2] [FeFe]- and [NiFe]hydrogenases afford striking natural examples of efficient catalytic devices in which the production or uptake of dihydrogen is catalyzed at bimetallic active sites.[3] In particular, one of the keys of the activity of the [FeFe]hydrogenases' subsite is the asymmetry of the dinuclear entity and the cooperativity of the two metal centers that play different roles. One iron moiety (distal) is involved in the H^+/H_2 conversion process, and the other (proximal) acts as a metalloligand bearing a redox ligand.[4] Numerous studies of bioinspired diiron carbonyl models have led to the definition of a general scheme, at the molecular level, for the functioning of this organometallic assembly.[5] Hexacarbonyl precursors $[Fe_2(CO)_6\{\mu\text{-dithiolate}\}]$, have afforded a readily accessible platform for synthesizing a large series of models, but the design of the first coordination sphere of the iron atoms in this class of molecules is limited to the substitution of carbon monoxide (CO) by better electron-donor groups, giving compounds of the general formula $[Fe_2(CO)_{6-x}L_x(S_2R)]$.[6] The formal replacement of one iron moiety in such a bimetallic entity by a metalloligand has been developed to afford models of the [NiFe]hydrogenases active site through a simple and powerful synthetic strategy[7] that has been recently extended to the design of novel FeCo and FeMn heterobimetallic molecules.[8] In order to assess how the reactivity of an iron center of a bimetallic species might be modulated through the neighboring metal atom, we decided to extend our work on dissymmetrically substituted homodinuclear bioinspired iron molecules[9] to heterobimetallic complexes. Because of our continuing interest in chemical nitrogen fixation processes,[10] we opted for a new FeMo heterobimetallic system that would model a truncated $\{FeMoS_2\}$ part of the FeMo cofactor of nitrogenase.[11]

For this purpose, the complex $[FeMo(CO)_5(\kappa^2\text{-dppe})(\mu\text{-pdt})]$ (**1**; dppe = 1,2-bis(diphenylphosphino)ethane and pdt^{2-} = 1,3-propanedithiolate) was synthesized in moderate yield (~50%), at room temperature, by reacting two mononuclear precursors, $[Fe(CO)_2(\kappa^2\text{-dppe})(\kappa^2\text{-pdt})]$ and $[Mo(CO)_3(CH_3CN)_3]$, using the synthetic strategy recently reported by Rauchfuss and co-workers for NiFe heterobimetallic systems[7] (see the procedure in the Supporting Information, SI).

1 was characterized by elemental analyses, IR, NMR, and Mössbauer spectroscopies, and X-ray analysis. The IR spectrum of **1** in CH_2Cl_2 (Figure S1 in the SI) has four characteristic bands in the ν(CO) region, 2016 (s), 1936 (s), 1882 (s), and 1850 (m) cm^{-1}, suggesting the presence of terminal and semibridging CO ligands. The $^{31}P\{^1H\}$ NMR spectrum in $CDCl_3$ (Figure S2 in the SI) shows a singlet at 60.8 ppm assigned to the two phosphorus atoms of the diphosphine, which suggests their equivalence. This can be related to dibasal coordination of dppe at the iron atom. No dynamic process, usually associated with the dppe and pdt groups, was detected by variable-temperature $^{31}P\{^1H\}$ NMR studies in the range 25−80 °C.[9a] The ^1H NMR spectrum of **1** in $CDCl_3$ (Figure S3 in the SI) and 2D COSY $^1H-^1H$ NMR experiments (Figure S4 in the SI) allowed the assignment of all of the expected signals associated with the phenyl, dppe, and pdt groups. The recording of the $^{13}C\{^1H\}$ NMR spectrum in $CDCl_3$ (Figure S5 in the SI) revealed, in the carbonyl region, the presence of four resonances appearing as a singlet at 229.1 ppm, a triplet at 219.8 ppm with a coupling constant of 16.5 Hz ($^2J_{PC}$), and two singlets in a 2:1 ratio at 213.9 and 203.1 ppm, respectively. This pattern suggests a $\{Fe(CO)P_2\}(\mu\text{-CO})\{Mo(CO)_3\}$ core for **1**, in agreement with the X-ray results (Figure 1a). The molybdenum atom lies in a pseudooctahedral geometry,

Received: July 31, 2014
Published: October 20, 2014

   dx.doi.org/10.1021/ic501875q | *Inorg. Chem.* 2014, 53, 11345−11347

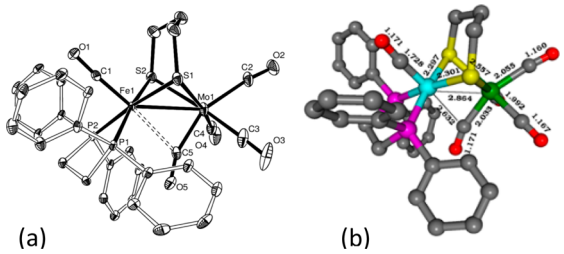

Figure 1. (a) ORTEP view (ellipsoids at the 30% probability level) of **1**. (b) Schematic representation of the calculated structures of **1**, with selected geometrical parameters.

and the iron atom is in a typical square-pyramidal geometry, supplemented by an interaction with a semibridging CO [C5–Fe1, 2.514(8) Å; C5–Mo1, 1.987(6) Å; O5C5Mo1, 160.6(5)°; C5–Mo1–Fe1, 60.99(17)°]. The Fe–Mo distance [2.7795(8) Å] suggests a Fe–Mo bond.[12] The Mo–C(O) distance of the apical CO coordinated to molybdenum is significantly longer than those of the equatorial CO ligands, suggesting a potential reactivity based on the lability of this carbonyl group. ^{13}CO-labeling studies were also performed and suggested intramolecular transfer of a CO ligand from the iron framework to the molybdenum atom, giving the observed {Mo(CO)$_4$} moiety (Figures S6–S8 in the SI).

Mössbauer spectroscopy and density functional theory (DFT) calculations were performed in order to gain deeper insight into the electronic and structural properties of **1** and to address the question of the best electronic description of this {Fe–Mo} entity.

Figure 2 reproduces the 4.2 K Mössbauer spectra recorded on a powder sample of **1**. They can be nicely simulated, assuming a

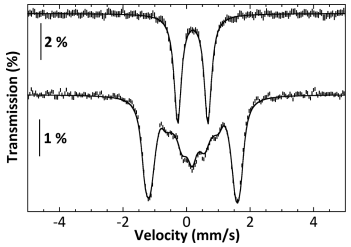

Figure 2. Experimental Mössbauer spectra recorded at 4.2 K with a 60 mT (top) or 7 T (bottom) external magnetic field parallel to the γ-rays (hatched marks). Simulated spectra using the parameters listed in Table S1 are shown as solid lines.

single iron site within a diamagnetic species with the following parameters: $\delta = 0.20$ mm/s, $\Delta E_Q = -0.95$ mm/s, $\eta = 0$, and $\Gamma_{fwhm} = 0.27$ mm/s. Despite the lack of reliable correlation with the oxidation state of the iron atom owing to the strong π-backbonding of the ligands,[13] the δ value may be compared to that of similar complexes. Note that small variations are observed due to substitution of CO by phosphine.[14]

The δ value in **1** is larger than that found for the Fe^{II} ion in the [Fe^{I}Fe^{II}(μ-dithiolato)(μ-CO)]$^+$ core-complexes[15] or that for low-spin Fe^I ions in homovalent diiron Fe^{I}Fe^I [15a,c,16] or iron–nickel Fe^{I}Ni^I [17] complexes. It is more similar to that of low-spin Fe^I site in mixed-valent Fe^{I}Fe^{II} [15] or Fe^{I}Ni^{II} [14] complexes. In an attempt to conclude on the oxidation state of the metal ions in **1**, DFT calculations were thus performed.

The geometrical parameters of **1**, calculated by DFT, are in good agreement with those of the crystallographic structure (Figure 1b). In addition, **1** is more stable than the isomer featuring the basal–apical coordination of the diphosphine ligand by about 8 kcal/mol. Calculated vibrational frequencies corresponding to the CO stretching modes are also in close agreement with the experimental values (Figure S9 in the SI). The calculated Mössbauer parameters of **1** ($\delta = 0.22$ mm/s, $\Delta E_Q = -0.86$ mm/s and $\eta = 0.87$) (Table S1 in the SI) match nearly perfectly the experimental values, suggesting that the computational scheme is able to describe correctly the electronic structure of **1**. The parameters of the Mössbauer spectra of complexes [FeFe(CO)$_4$(PMe$_3$)$_2$(μ-dmpdt)]$^{0/+}$ (**2**/**2**$^+$; dmpdt^{2-} = 2,2-dimethyl-1,3-propanedithiolate)[15a,b] were calculated as references of Fe^{I}Fe^I and Fe^{I}Fe^{II} redox states, to check the validity of calculations, and satisfying results were obtained (Table S2 in the SI). Metal atomic charges are not always reliable to evaluate the redox state of metals in clusters like **1** because only very small changes are observed when ligands are replaced or when the net charge of the cluster is changed because of the covalent bond character and the π acidity of the CO ligands. Analysis of the electronic structure can be more insightful when considering the net charges of the three subunits {(dppe)(CO)Fe}, {pdt}, and {Mo(CO)$_4$} (see Figure S10). Remarkably, the charge of the {(dppe)(CO)Fe} fragment (+0.68 au) is more than 1 au more positive than that of the {Mo(CO)$_4$} fragment (−0.51 au), while the {pdt} fragment in the complex have a small negative charge (−0.17 au). The same analysis has also been performed for **2**, for which, as expected, the charges of the two iron fragments are very similar (Figure S10). The large charge separation of the two metal fragments in **1** suggests that this cluster can be better described as a Fe^{II}Mo^0 complex, rather than Fe^{I}Mo^I, with a dative bond between molybdenum and iron. Indeed, the calculated Wiberg bond index, equal to 0.22, indicates a metal–metal bond.

The large charge separation in **1** can be rationalized with an orbital diagram obtained by dividing the cluster into the two neutral {(dppe)(CO)(pdt)Fe} and {Mo(CO)$_4$} subunits, which feature the formal Fe^{II} and Mo^0 redox states, respectively (Figure 3). Formation of the metal–metal bond in **1** from the two fragments might be described as a donor–acceptor interaction between the highest occupied molecular orbital (HOMO) of {Mo(CO)$_4$} and lowest unoccupied molecular orbital (LUMO) of {(dppe)(CO)(pdt)Fe} (for the detailed orbital analysis, see

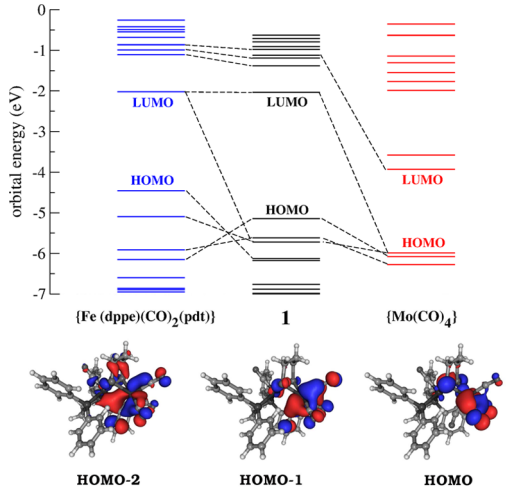

Figure 3. Orbital diagram and relevant frontier molecular orbitals of **1** calculated at the B3LYP/TZVP level of theory on the geometries optimized using the BP86/TZVP scheme.

dx.doi.org/10.1021/ic501875q | Inorg. Chem. 2014, 53, 11345–11347

Figure S11 in the SI). However, the HOMO of $\{Mo(CO)_4\}$ is much lower in energy than the LUMO of {(dppe)(CO)(pdt)-Fe}, unlike, for example, in **2** (Figure S12 in the SI). These two orbitals interact in a bonding combination, giving the HOMO−2 in **1**, which, due because of the large energy separation, is strongly localized on the molybdenum site, as is also shown by the atomic contributions to the orbital population reported in Table S3 in the SI. The HOMO and HOMO−1 in **1** roughly correspond to the HOMO−1 and HOMO−2 of the $\{Mo(CO)_4\}$ fragment and remain localized on this part of the molecule. This orbital analysis further supports a picture in which the $Fe^{II}Mo^0$ resonant form gives a significant contribution to the proper representation of the electronic structure of **1**. The Fe^{II} site in **1** can be compared to that in $\mathbf{2}^+$. The larger δ value obtained in **1** may be related to the longer distance in **1** between the iron site and the semibridging carbonyl group (Figure S13 in the SI). On the other hand, the electron density located between the two metal sites in the HOMO−2 may contribute to the high value of δ, which is more consistent with that of an Fe^I site.

The cyclic voltammetry of **1** at moderate scan rate (v = 1 V/s; Figure S14 in the SI) shows that it undergoes quasi-reversible one-electron reduction and oxidation steps in CH_2Cl_2−$[NBu_4][PF_6]$ ($E_{1/2}^{red}$ = −1.84 V; $E_{1/2}^{ox}$ = 0.12 V; potentials are versus Fc^+/Fc). At lower scan rates (0.05 V/s ≤ v < 1 V/s), **1** decreases according to an ECE-type mechanism, as shown by the fact that the current function, $i_p^{red}/v^{1/2}$, increases significantly with decreasing v (Figure S15 in the SI). Detailed studies of the electrochemical behavior of **1** under different experimental conditions (scan rates, solvent, and acidity) will be reported later on.

In summary, we describe in this Communication a novel FeMo heterobimetallic species that may be a promising platform to investigate the activation of resource molecules.

■ ASSOCIATED CONTENT

Supporting Information

CIF file, details on instrumentation, methods, synthetic procedures, and spectroscopic and crystallographic data of **1**. This material is available free of charge via the Internet at http://pubs.acs.org.

■ AUTHOR INFORMATION

Corresponding Authors

*E-mail: genevieve.blondin@cea.fr.
*E-mail: maurizio.bruschi@unimib.it.
*E-mail: schollha@univ-brest.fr.

Notes

The authors declare no competing financial interest.

■ ACKNOWLEDGMENTS

The Centre National de la Recherche Scientifique (CNRS), Université de Bretagne Occidentale (UBO), Université Joseph Fourier, Grenoble-1, the Agence Nationale de la Recherche (ANR-11-LABX-0003-01), and University of Milano-Bicocca are acknowledged for financial support.

■ REFERENCES

(1) (a) Adams, R. D.; Cotton, F. A. *Catalysis by Di- and Polynuclear Metal Cluster Complexes*; Wiley-VCH: New York, 1998. (b) Pétillon, F. Y.; Schollhammer, P.; Talarmin, J.; Muir, K. W. *Coord. Chem. Rev.* **1998**, *178*−*180*, 203−247.

(2) (a) Ritleng, V.; Chetcuti, M. J. *Chem. Rev.* **2007**, *107*, 797−858. (b) Wong, W.-T. *Comprehensive Organometallic Chemistry III*; Pergamon Press: Oxford, U.K., 2007; Vol. 6, pp 319−352.

(3) Lindhal, P. A. *J. Inorg. Biochem.* **2012**, *106*, 172−178.

(4) (a) Simmons, T. R.; Berggren, G.; Bacchi, M.; Fontecave, M.; Artero, V. *Coord. Chem. Rev.* **2014**, *270*−*271*, 127−150. (b) Gloaguen, F.; Rauchfuss, T. B. *Chem. Soc. Rev.* **2009**, *38*, 100−108. (c) Tard, C.; Pickett, C. J. *Chem. Rev.* **2009**, *109*, 2245−2274.

(5) (a) Capon, J.-F.; Gloaguen, F.; Pétillon, F. Y.; Schollhammer, P.; Talarmin, J. *C. R. Chimie* **2008**, *11*, 842−851. (b) Capon, J.-F.; Gloaguen, F.; Pétillon, F. Y.; Schollhammer, P.; Talarmin, J. *Coord. Chem. Rev.* **2009**, *253*, 1476−1494.

(6) (a) Darensbourg, M. Y.; Weigand, W. *Eur. J. Inorg. Chem.* **2011**, 994−1004. (b) Tschierlei, S.; Ott, S.; Lomoth, R. *Energy Environ. Sci.* **2011**, *4*, 2340−2352. (c) Wang, N.; Wang, M.; Chen, L.; Sun, L. *Dalton Trans.* **2013**, *42*, 12059−12071.

(7) Barton, B. E.; Whaley, M.; Rauchfuss, T. B.; Gray, D. L. *J. Am. Chem. Soc.* **2009**, *131*, 6942−6943.

(8) (a) Gao, H.; Huang, J.; Chen, L.; Liu, R.; Chen, J. *RSC Adv.* **2013**, *3*, 3557−3565. (b) Caroll, M. E.; Chen, J.; Gray, D. E.; Lansing, J. C.; Rauchfuss, T. B.; Schilter, D.; Volkers, P. I.; Wilson, S. R. *Organometallics* **2014**, *33*, 858−867.

(9) (a) Capon, J.-F; Gloaguen, F.; Pétillon, F. Y.; Schollhammer, P.; Talarmin, J. *Eur. J. Inorg. Chem.* **2008**, 4671−4681. (b) Munery, S.; Capon, J.-F.; De Gioia, L.; Elleouet, C.; Greco, C.; Pétillon, F. Y.; Schollhammer, P.; Talarmin, J.; Zampella, G. *Chem.—Eur. J.* **2013**, *19*, 15458−15461. (c) Ezzaher, S.; Capon, J.-F.; Gloaguen, F.; Pétillon, F. Y.; Schollhammer, P.; Talarmin, J. *J. Electronal. Chem.* **2009**, *626*, 161−170.

(10) Le Goff, A.; Vénec, D.; Le Roy, C.; Pétillon, F. Y.; Schollhammer, P.; Talarmin, J. *Inorg. Chem.* **2014**, *53*, 2200−2210.

(11) (a) Spatzal, T.; Aksoyoglu, M.; Zhang, L.; Andrade, S. L. A.; Schleicher, E.; Weber, S.; Rees, D. C.; Einsle, O. *Science* **2011**, *334*, 940−940. (b) Durrant, M. C. *Inorg. Chem. Commun.* **2001**, *4*, 60−62. (c) Henderson, R. A. *Chem. Rev.* **2005**, *105*, 2365−2437.

(12) Hsiano, S.-M.; Shyu, S.-G. *Organometallics* **1998**, *17*, 1151−1154.

(13) Gütlich, P.; Bill, E.; Trautwein, A. X. *Mössbauer Spectroscopy and Transition Metal Chemistry. Fondamentals and Applications*; Springer-Verlag: Berlin, 2011.

(14) Chen, D.; Ahrens-Botzong, A.; Schünemann, V.; Scopelliti, R.; Hu, X. *Inorg. Chem.* **2011**, *50*, 5249−5257.

(15) (a) Hsieh, C.-H.; Erdem, O. F.; Harman, S. D.; Singleton, M. L.; Reijerse, E. J.; Lubitz, W.; Popescu, C. V.; Reibenspies, J. H.; Brothers, S. M.; Hall, M. B.; Darensbourg, M. Y. *J. Am. Chem. Soc.* **2012**, *134*, 13089−13102. (b) Silakov, A.; Olsen, M. T.; Sproules, S.; Reijerse, E. J.; Rauchfuss, T. B.; Lubitz, W. *Inorg. Chem.* **2012**, *51*, 8617−8628. (c) Stoian, S. A.; Hsieh, C.-H.; Singleton, M. L.; Casuras, A. F.; Darensbourg, M. Y.; McNeely, K.; Sweely, K.; Popescu, C. V. *J. Biol. Inorg. Chem.* **2013**, *18*, 609−622.

(16) (a) Le Cloirec, A.; Best, S. P.; Borg, S.; Davies, S. C.; Evans, D. J.; Hughes, D. L.; Pickett, C. J. *Chem. Commun.* **1999**, 2285−2286. (b) Razavet, M.; Davies, S. C.; Hughes, D. L.; Barclay, J. E.; Evans, D. J.; Fairhurst, S. A.; Liu, X.; Pickett, C. J. *Dalton Trans.* **2003**, 586−595. (c) Tard, C.; Liu, X.; Ibrahim, S. K.; Bruschi, M.; De Gioia, L.; Davies, S. C.; Yang, X.; Wang, L.-S.; Sawers, G.; Pickett, C. J. *Nature* **2005**, *433*, 610−613.

(17) Schilter, D.; Nilges, M. J.; Chakrabarti, M.; Lindahl, P. A.; Rauchfuss, T. B.; Stein, M. *Inorg. Chem.* **2012**, *51*, 2338−2348.